

TUNNELING AND INFRARED SPECTROSCOPY ON HIGH T_c SUPERCONDUCTORS

J. HARTGE¹, L. FORRO²⁺, D. MANDRUS^{1*}, MICHAEL C. MARTIN¹, C. KENDZIORA¹
and L. MIHALY¹

¹ Department of Physics, State University of New York, Stony Brook NY, 11794-3800

² Ecole Polytechnique Federale de Lausanne, CH 1015 Lausanne, Switzerland

ABSTRACT - We have investigated single crystals of $\text{Bi}_2\text{Sr}_2\text{Ca}_{1-x}\text{Y}_x\text{Cu}_2\text{O}_8$ ($x=0 - 0.35$) by far infrared transmission spectroscopy and by break junction tunneling. The junctions were made at low temperatures in vacuum, and SIS tunneling was measured at various temperatures and magnetic fields. The tunneling results are interpreted in terms of a Josephson current and a single electron tunneling density of states (DOS). Although the DOS is found to be zero at the Fermi level, we do not see a fully developed gap even at temperatures well below the critical temperature. There is qualitative agreement between tunneling and infrared spectroscopy results.

Keywords: tunneling, gap, Josephson current, infrared spectroscopy

INTRODUCTION

Tunneling and microwave spectroscopy proved to be among the most effective methods of exploring the properties of superconductors (Tinkham 1975, Wolf 1985). For the high temperature superconductors the strong structural anisotropy and the short coherence length, combined with the chemical variability of the materials, presents special difficulties in tunneling and far infrared optical measurements. We developed a method to make thin single crystals of a series of compounds with nominal composition $\text{Bi}_2\text{Sr}_2\text{Ca}_{1-x}\text{Y}_x\text{Cu}_2\text{O}_8$, and the use of these samples enabled us to overcome some of these difficulties. Here we summarize the results obtained over the past few years and we report on the most recent developments (Forro *et al.* 1990a, Mandrus *et al.* 1991a, 1993a, 1993b).

Break junction tunneling, pioneered by Moreland (Moreland 1985; for recent results see Muller *et al.* 1992) provides a way to study clean junctions, prepared *in situ* at low temperatures. We made reproducible break junctions and we measured the superconductor-insulator-superconductor (SIS) tunneling characteristics of the $\text{Bi}_2\text{Sr}_2\text{CaCu}_2\text{O}_8$ compound. We tested junctions obtained by breaking parallel and perpendicular to the copper oxide planes (tunneling perpendicular and parallel to the *c*-axis of the crystal, respectively), and we found that the tunneling curves obtained in the two directions are different. For *c*-axis tunneling the voltage and temperature dependence can be well described by a logarithmic function. The tunneling conductance does not show major features as the superconducting transition is crossed. For *a-b* plane tunneling (electrons moving parallel to the CuO planes) the superconducting transition is clearly visible, with features on an energy scale of 50 meV. The junctions proved to be surprisingly robust, and they survived exposure to rather high voltages and current densities as long as they were kept at low temperatures. The large bias behavior of the junctions is well described by conventional tunneling theory, with reasonable junction width and barrier height. At zero bias the junctions exhibit Josephson current. This feature depends on the magnitude and direction of the external magnetic field.

The optical transmission of conventional *s*-wave superconductors shows a peak around, or somewhat above the gap frequency (Tinkham 1975). In high T_c superconductors the larger energy scales, combined with the low (Kamaras *et al.* 1990) and temperature dependent (Nuss *et al.* 1991, Romero *et al.* 1992, Bonn *et al.* 1992) relaxation rate of the normal charge carriers may conspire to hide this feature. For the study reported here the relaxation rate was intentionally enhanced, but the transmission peak was still not seen. We found a general, qualitative agreement between the tunneling and infrared transmission results, although neither is consistent with an isotropic *s*-wave superconductor.

EXPERIMENTAL METHOD

Single crystals of $\text{Bi}_2\text{Sr}_2\text{CaCu}_2\text{O}_8$, $\text{Bi}_2\text{Sr}_2\text{Ca}_{1-x}\text{Y}_x\text{Cu}_2\text{O}_8$, and other doped compounds of the same family have been grown by the conventional flux method (Forro *et al.* 1990b). The structure and composition of the crystals have been characterized (Kendziora *et al.* 1992), and the electrical and thermal transport properties have been measured in great detail (Mandrus *et al.* 1991b, Forro *et al.* 1990c). The tunneling measurements reported here were performed on the "pure" compound of nominal composition $\text{Bi}_2\text{Sr}_2\text{CaCu}_2\text{O}_8$; the "dirty" samples were used in the optical studies.

Thin single crystals of about $0.5\text{mm} \times 0.5\text{mm} \times 1000\text{\AA}$ were cleaved from the bulk (Forro *et al.* 1990a, 1990b). The "as grown" crystals had superconducting transition temperatures ranging from 60K to 80K. The crystals were subjected to a heat treatment in air at 600C. This treatment established a higher oxygen concentration in the crystals, and brought T_C close to or above 90K. Nevertheless, even after the heat treatment, small variations of the critical temperature were observed for $\text{Bi}_2\text{Sr}_2\text{CaCu}_2\text{O}_8$ crystals obtained from different batches; this is most likely due to minor variations in the cation composition and oxygen content.

For *a-b* plane tunneling measurements the samples are glued on a thin piece of insulating $\text{Bi}_2\text{Sr}_2\text{YCu}_2\text{O}_8$. The mechanical properties of this material are close to $\text{Bi}_2\text{Sr}_2\text{CaCu}_2\text{O}_8$, and therefore it serves well as a protection against thermally induced breaks during the cooling. The $\text{Bi}_2\text{Sr}_2\text{YCu}_2\text{O}_8$ is varnished on an elastic strip of metal, and the electrical contacts are made to the $\text{Bi}_2\text{Sr}_2\text{CaCu}_2\text{O}_8$ using silver paste and $12\mu\text{m}$ gold wires. (In most cases we used two probes, since the junction resistance was high relative to the lead resistances. Occasionally we made four probe measurements, with similar results.) The assembly is cooled in vacuum or in low pressure He exchange gas, and the resistivity of the sample is monitored. Once at liquid He temperature, the metal strip is carefully bent in the middle until the sample breaks. At this point the resistance between the electrical contacts jumps from zero to infinity. Reducing the curvature of the strip restores the electrical contact, and we can modify the junction conductance by adjusting the pressure on the elastic strip. If not disturbed, the differential conductance curve of the junction is rather stable. Moderate changes in temperature (like warming up to 100K) lead to reversible modifications. Once the sample is warmed to room temperature the junction changes permanently, and the low temperature tunneling characteristics no longer resemble the original ones. Presumably, this is due to oxygen diffusion at the junction surface.

For the study of the Josephson current the whole assembly was placed in a superconducting magnet. We found that the magnetic forces (the torque acting on the non-spherical, anisotropic superconductor) can destroy the junction, but sometimes the large bias conductance was found to be independent of the magnetic field, indicating field-independent junction parameters. For these junctions the only field dependence appeared around zero bias and the tunneling curve reproduced well after the application of magnetic fields up to 2 Tesla. We studied two configurations: in the first one the magnetic field was parallel to the *c*-axis (*i.e.* the field lines were nominally perpendicular to the tunneling current), and in the second configuration the field was applied in the *a-b* plane, parallel to the current flow.

In the *c*-axis tunneling measurements, a thicker crystal was glued between two arms of a U-shaped metal strip. The superconducting transition was detected in the *c*-axis resistance of the sample. The crystal was cleaved *in-situ* by pushing the arms of the strip apart. The contact between the two pieces was established by decreasing the separation between the arms.

We inspected the junctions after removing them from the cryostat. We always found a clean break, running across the sample in the expected direction. However, the exact location of the junction cannot be determined. For *a-b* plane tunneling the junction is formed somewhere along the break line, whereas for *c*-axis tunneling it can be anywhere on the cleavage plane.

The low temperature, zero field, a - b plane tunneling was studied most extensively, on approximately 30 junctions. Five junctions were studied in magnetic field. Junctions were considered "good" if the interpolated zero-bias conductance was 20-100 times lower than the high bias value. (The interpolation was necessary to eliminate the influence of the Josephson current.) After this selection criterion was applied, the tunneling curves were reproducible. The c -axis tunneling was studied on two crystals. The junction parameters were varied by mechanical adjustment, in order to cover a wide range of resistances.

For the optical measurements, each sample was mounted over a hole in a copper plate (Forro *et al.* 1990a). Occasionally we used gold plated sapphire chips for the sample holder, so that the electrical resistivity of the sample could be measured simultaneously. The optical measurements discussed here were performed on "dirty" samples, but we also measured the material in the "pure" state (Forro *et al.* 1990a). In order to extract $\sigma(\omega) = \sigma_1 + i\sigma_2$, the complex optical conductivity, one needs to know the sample thickness, and one has to perform a Kramers-Kronig analysis (Tanner *et al.* 1991, Romero *et al.* 1992). However, valuable qualitative conclusions can be drawn from the transmission spectra alone, especially by simulating transmission curves with a hypothetical optical conductivity. We take this route in the present work.

OUT-OF-PLANE TUNNELING The tunneling in $\text{Bi}_2\text{Sr}_2\text{CaCu}_2\text{O}_8$ proved to be very anisotropic (Mandrus *et al.* 1991a). A typical set of c -axis conductance curves are presented in Fig. 1. The "bump" around 50mV, visible in the low temperature tunneling curve in the Figure, is weaker or totally missing for other junctions (Mandrus *et al.* 1991a). Apart from this feature the curves are smooth. For temperatures up to 100K the absolute value of the conductance at 200mV did not change significantly. At higher temperatures the junction conductance started to drift (probably due to thermal expansion). In Fig. 1 we plot the normalized conductance to compensate for the drift.

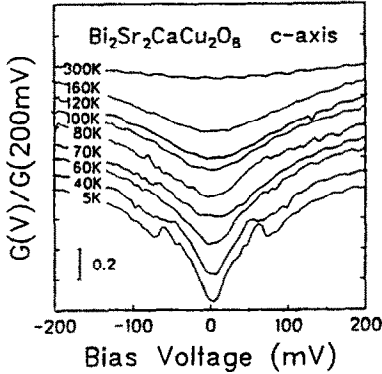


Fig. 1. Normalized tunneling conductance curves of a c axis junction for several temperatures, as indicated on the left side of the curves. For the 5K plot, the zero conductance coincides with the voltage axis, and the absolute value of the maximum conductance is $0.9(\text{k}\Omega)^{-1}$. Subsequent curves are shifted up by 0.1 unit each, for better visibility.

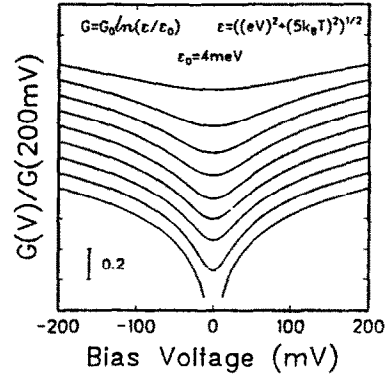


Fig. 2. A logarithmic function, described by Eq. (1), plotted the same way as the conductance curves of Fig. 1.

The temperature dependence of the conductance closely follows a logarithmic function. Furthermore, the voltage dependence at low temperature is also logarithmic (this feature has been confirmed for other junctions). The full behavior is well described by the function

$$G = G_0 \log \left\{ \sqrt{(5k_B T)^2 + (eV)^2} / \epsilon_0 \right\} \quad (1)$$

This function, with $\epsilon_0 = 4\text{meV}$, is plotted in Figure 2.

For break junctions it is very hard to prove that tunneling is actually happening at the junction, since little is known about the nature of the insulating layer. There is no convincing proof that the conductance curves of the *c*-axis junctions are indeed due to tunneling; it is possible that a weak link or constriction is formed. Nevertheless, it is interesting to note that logarithmic "zero bias anomalies" are common when the tunneling or constricted electrons are subjected to inelastic scattering. Examples are abundant in the literature ranging from tunneling *via* Kondo impurities (Mezei and Zawadowski, 1971) to two level systems in a normal metal weak link (Ralph and Buhrman, 1992).

Why should scattering be so important when the electrons move along the *c*-axis? The anisotropic band structure of these materials offers an explanation (Littlewood and Varma, 1992; see also Kirtley and Scalapino 1990). Due to the two-dimensional nature of the copper oxide layers, the electrons arrive at the junction at an angle of incidence close to 90° (*i.e.* the electrons move nearly parallel to the junction surface). There is a very little chance that tunneling will happen, since for non-zero incidence angle the tunneling probability cuts off rapidly. However, if the electron momentum is changed by scattering in the neighborhood of the junction, then the electron can tunnel, and be scattered again to an appropriate final momentum state. This "double scattering" is a second order process, but this is the *only* way that tunneling occurs in this anisotropic compound. Therefore *c*-axis tunneling is not a reflection of the bulk density of states, but is dominated by surface scattering processes, even if no impurities are placed in the junction intentionally.

The arguments provided above do not depend on the nature of the scattering, but the logarithmic voltage and temperature dependence of the experimental results can be best reconciled with inelastic processes, involving a very broad energy range, and leading to giant zero bias anomalies. It remains to be seen if the peculiarities of the crystal structure of this high temperature superconductor (like the apical oxygen above the CuO layers, the BiO layers exposed at the break surface, or possible two level systems due to the complexity of the unit cell (Zawadowski 1993) play a role here.

IN-PLANE TUNNELING

The signature of the superconducting state is expected to show up in the *a-b* plane tunneling results. Therefore we concentrated most of our efforts on this junction geometry. In particular, we established a degree of reproducibility between various junctions, we studied the temperature dependence and we attempted to clarify the direction of the tunnel current by investigating the magnetic field dependence of the Josephson component. The early studies have been reported in (Mandrus *et al.* 1991a). More recently, Becherer and co-workers reproduced some of our results (Becherer *et al.* 1992).

A typical set of tunneling curves for the *a-b* plane junction is shown in Fig. 3. The density of states $N(E)$, shown in Fig. 4, was evaluated by deconvolving

$$I = A \int N(E) N(E+eV) \{f(E) - f(E+eV)\} dE \quad (2)$$

Here A is the tunneling probability, assumed to be independent of the applied voltage V and the electronic energy E , I is the current, and f is the Fermi function. Some features of this density of states, like the linear behavior around the Fermi energy, the downward slope at large bias and the conservation of electronic states as a function of temperature were discussed earlier (Mandrus *et al.* 1993b).

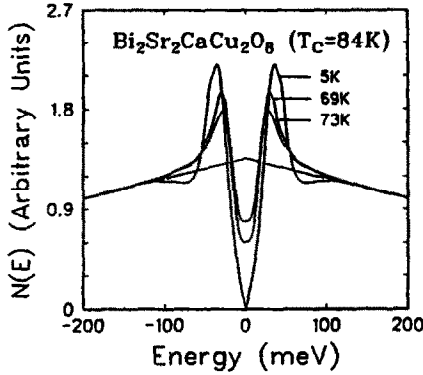


Fig. 3. Conductance of an *ab* plane junction at several temperatures below T_c . The conductance becomes a smooth function of voltage above the superconducting transition.

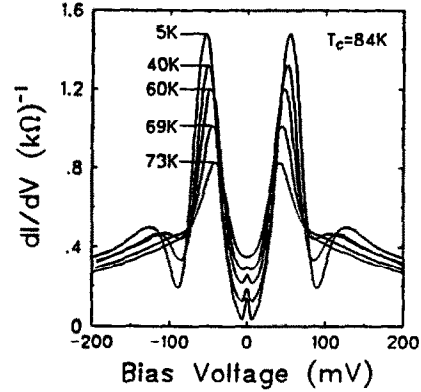


Fig. 4. Tunneling density of states evaluated by using Eq. (2) and the measurements presented in Fig. 3.

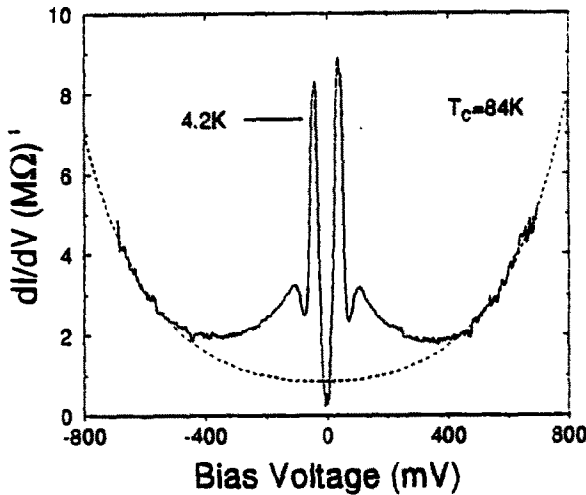


Fig. 5. Tunneling conductance over a wider voltage range for an *ab* plane junction. The upturn at larger voltages was interpreted in terms of Eq. (3). The fit is represented by the dotted line.

The large bias behavior is illustrated on another junction in Fig. 5. The voltage on this junction was swept several times to high values, and the entire tunneling curves were reproduced, indicating no drastic heating or breakdown effects. We note that attempts to do similar sweeps on junctions of low resistance were not successful; the junction was permanently damaged at large bias voltages. The upturn at larger voltage is due to the deformation of the potential barrier when the applied bias becomes comparable to the barrier height (Brinkman *et al.* 1970). According to a simple tunneling model (Burstein 1969), the differential conductance at large bias should behave as

$$G = C E_0 \cosh \{eV/E_0\} \quad (3)$$

$$E_0(V) = \hbar/\sqrt{2m} \sqrt{\Phi - eV/2} / w$$

with three fitting parameters: junction thickness w and barrier height Φ and an overall scale factor C . The dotted line in the Figure corresponds to this expression with $w = 13$ Angstrom and $\Phi = 1.2$ eV. Note that the fit is non-trivial, since a constant and a quadratic term in the voltage is not sufficient. Beyond the fourth order term the uniqueness of the fit cannot be proven, but Eq.(3) is not expected to be appropriate for higher order terms (Burstein, 1969). The junction parameters obtained from the fit are very reasonable, lending support to the claim that the features seen in Fig. 4. are indeed due to tunneling.

SIS junctions are expected to exhibit Josephson current. In our *a-b* plane conductance curves this shows up as a small peak at zero bias, but the Josephson current is better seen in direct I-V measurements. In Fig. 6. the zero bias behavior of a selected junction is shown. The Josephson contribution does not look like a textbook example, but it is clearly visible. This measurement was done in a two probe configuration and the finite lead resistance resulted in a finite slope at $V=0$ (ideally, the current should increase without observable voltage drop). One expects a sharp switch to zero Josephson current - in our case there is a rounding due to instrumental noise. Finally, we have an observable single electron contribution to the total current. This can be best subtracted by interpolating the I-V curve from the higher bias parts. The interpolation is indicated by the solid line in the Figure. (We used a linear and a cubic term. At zero bias the ohmic contribution, represented by the linear term, is 1/20 of the large bias conductance of the junction. This fraction is larger than the typical zero-bias conductance of our junctions)

The junction was placed in a magnetic field parallel to the *c*-axis (that is the magnetic field is supposed to thread the junction perpendicular to the current flow). In planar junctions of homogeneous current density the Josephson current is expected to show the well known "interference" pattern as a function of the magnetic field. Our junctions are not so well defined, and the current density is likely to have a bell-shaped distribution. Therefore the Josephson current decays monotonically as a function of field. Figure 7. was constructed by reading out the Josephson current from I-V characteristics like those plotted in Fig. 6. At the magnetic field corresponding to the half maximum of the curve, the junction area contains about 1/2 magnetic flux quantum. The junction area is defined as $(2\lambda + w)l$, where λ is the magnetic penetration depth, l is the linear dimension of the junction and $w \ll \lambda$ is the barrier width. Assuming that the external field equals the field in the junction we estimate a size $l \approx 1000$ Angstrom. Since the expulsion of magnetic field by the superconductor increases the flux through the junction, this value can serve only as an upper limit.

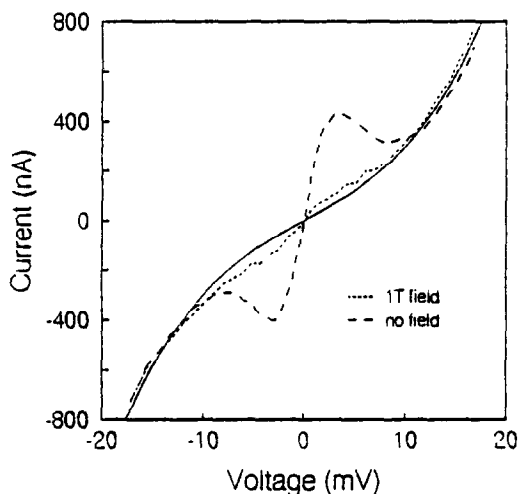


Fig. 6. I-V characteristics of an *ab* plane junction around zero bias at zero and 1.5 Tesla magnetic field applied parallel to the *c* axis. The Josephson contribution is clearly visible, and it is suppressed at high fields. The solid line represents the single electron contribution, obtained by fitting to the curve at larger bias voltages.

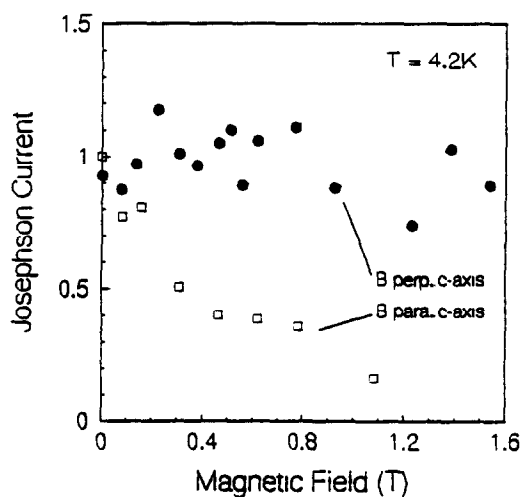


Fig. 7. Magnetic field dependence of the Josephson current for two different junctions. The Josephson current is normalized to its zero field value. Squares represent a measurement when the field was applied perpendicular to the current flow; the zero field Josephson current is 400nA, as seen in Fig. 6. For circles the field is parallel to the current, and the Josephson current is 50nA.

We carried out similar experiments on another junction, with magnetic field oriented perpendicular to the *c*-axis (parallel to the current flow). The results are also shown in Fig 7.

There was no observable decay of the Josephson current. The significance of these experiments is to indicate that the junction surface is indeed perpendicular to the a - b planes, as expected from the macroscopic configuration of the break.

OPTICAL TRANSMISSION

In search of the transmission peak originally observed by Tinkham and co-workers (Tinkham, 1975), we performed far infrared spectroscopy on thin $\text{Bi}_2\text{Sr}_2\text{CaCu}_2\text{O}_8$ single crystals. The measurements were carried out at the U4IR beamline of the National Synchrotron Light Source at the Brookhaven National Laboratory (Ferro *et al.* 1991a, Mandrus *et al.* 1993a).

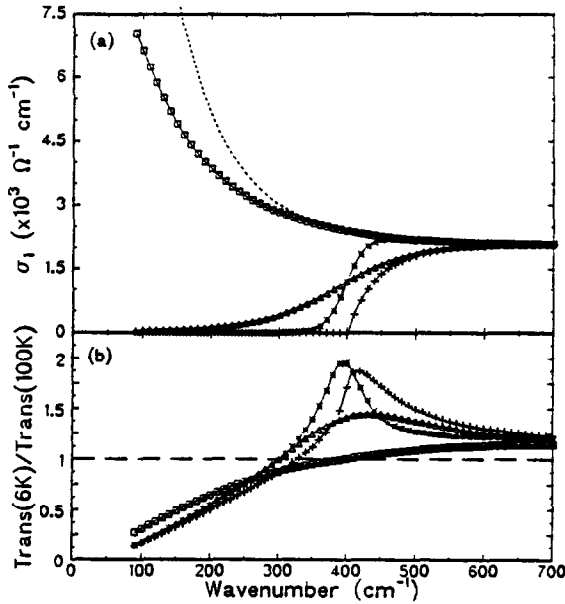


Fig. 8. Real part of the optical conductivity (upper panel) and infrared transmission (lower panel) for simulated "superconductors at 5K". The dotted line in the upper panel represents the "normal state at 100K", and the corresponding transmission function was used to normalize the transmission in the superconducting state.

The transmission peak of thin superconducting films is due to a dip in σ_2 which, in turn, is related to the sharp onset in σ_1 at frequency $\hbar\omega=2\Delta$. This is illustrated in Fig. 8., where we plot several $\sigma_1(\omega)$ functions and the corresponding transmission curves, assuming a sample thickness of 1000 Angstrom (Mandrus *et al.* 1993a). The normal state conductivity is indicated by the dotted line in the Figure. For the superconducting state the conductivity curves were chosen to mimic various possibilities: sharp gap at 400 cm^{-1} , smeared gap and gapless transfer of oscillator strength from finite frequency to zero frequency. In each case the missing area was calculated, the appropriate Dirac delta function was added at zero frequency, and Kramers Kronig transform was performed to obtain the imaginary part, σ_2 . The transmission of a film was expressed in terms of the thickness d and the complex optical conductivity using

$$t = \frac{4N}{(N+1)^2 \exp(-i\eta) - (N-1)^2 \exp(i\eta)} \quad (4)$$

where $N = \sqrt{1+i4\pi\sigma/\omega}$ is the complex index of refraction and $\eta = 2\pi \omega N d$, and $|t|^2$ is the transmitted power fraction. We used this expression to calculate the transmission ratio of the superconducting to the non-superconducting state.

In the calculations described above we made the implicit assumption that the scattering processes leading to the particular frequency dependence of $\sigma(\omega)$ in the normal state will not change when we move to the superconducting state. This assumption is put into question again by the recent microwave experiments of Bonn *et al.* (1992). In terms of a two fluid model their observation can be viewed as a dramatic drop in the relaxation rate of the normal component below T_c . This experiment brings up again the so called "clean limit" arguments originally applied to high T_c materials by Kamaras *et al.* (1990): The infrared radiation cannot

distinguish a superconductor from a very good metal, and if the relaxation rate of the normal component is small enough, the infrared optical properties will not show evidence for the gap.

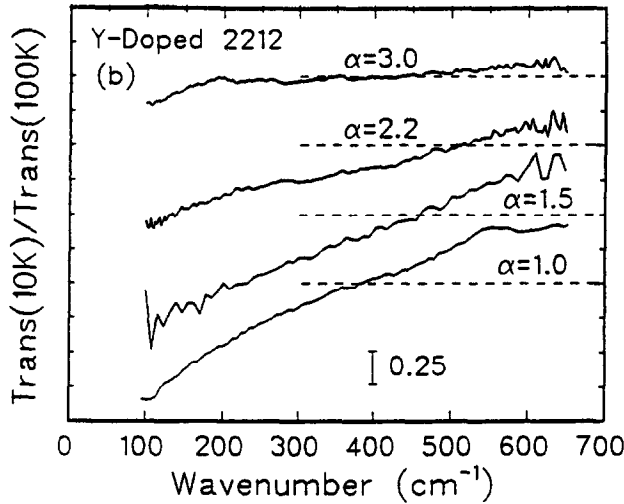


Fig. 9. Far infrared transmission of variously doped $\text{Bi}_2\text{Sr}_2\text{Ca}_{1-x}\text{Y}_x\text{Cu}_2\text{O}_8$ crystals. All curves are normalized to the transmission at 100K. The samples are about 1000 Angstrom thick. The curves are shifted in the vertical direction for better view; the dotted lines provide the transmission ratio = 1 reference.

To avoid the "the catch of clean limit", we performed a series of experiments on various impure samples, where the relaxation rate of the normal carriers was intentionally enhanced. Presumably, the impurities enhancing the relaxation rate in the normal state will do so in the superconducting state as well, and the normal component will not slide into the clean limit. In fact, the calculated curves plotted in Fig 8. were produced by assuming that the relaxation rate is entirely independent of the temperature.

The experiments were performed on a series of $\text{Bi}_2\text{Sr}_2\text{Ca}_{1-x}\text{Y}_x\text{Cu}_2\text{O}_8$ crystals. The impurity content of the samples was characterized by the resistivity ratio at 300K, $\alpha = \rho_{\text{dirty}}/\rho_{\text{pure}}$. The impurity contribution to the scattering in the material of $\alpha=1.5$

corresponds to approximately 50% of the room temperature scattering rate in the clean compound. For higher doping levels the variation in carrier concentration becomes also significant, accompanied by a reduction of the critical temperature (Kendziora *et al.* 1992).

The results are shown in Fig. 9. There is no visible peak in any of the curves (the "bump" around 600cm^{-1} in the pure, $\alpha=1$, sample was not reproducible). The comparison to Fig. 8. illustrates that the superconducting gap does not show up in the frequency range corresponding to $2k_B T_C - 10 k_B T_C$, even if the scattering rate is enhanced and the material is not in the clean limit. Similar studies on electron irradiated, heavy ion irradiated crystals, and oxygen deficient (heat treated in vacuum) samples, lead to the same results (Mandrus *et al.* 1993a).

CONCLUSIONS

We used two traditionally very successful tools, tunneling and transmission spectroscopies to search for the superconducting gap and to find the density of states in the superconducting state. We found no sharp gap in either of these studies, indicating that the high T_C compound $\text{Bi}_2\text{Sr}_2\text{CaCu}_2\text{O}_8$ has no isotropic *s*-wave ground state. Both sets of data are compatible with a *d*-wave, or with very anisotropic *s*-wave state. If an anisotropic gap function is assumed at zero temperature, then the tunneling data provide $\Delta_{\text{max}} = 38$ meV for the maximum value of the gap. For anisotropic *s* wave superconductivity the minimum gap may not exceed $\Delta_{\text{min}} = 2$ meV (deduced from the experimental uncertainty due to the Josephson current). The linear tunneling density of states around the E_F , and the peak in the DOS at an unusually high energy (38meV, corresponding to $\approx 10k_B T_C$), is also a signature of the anisotropic gap.

In a tetragonal crystal the optical spectroscopy cannot explore the gap anisotropy within the *a-b* plane, because the general symmetry properties of the lattice lead to isotropic optical conductivity. Although $\text{Bi}_2\text{Sr}_2\text{CaCu}_2\text{O}_8$ is not perfectly tetragonal, there is only a small difference in the optical conductivity between the *a* and *b* directions (Romero *et al.* 1992). Therefore the optical transmission is not expected to distinguish an anisotropic gap from a

truly gapless behavior. There is ample evidence for the transfer of spectral weight from finite frequencies to the superconducting condensate; what is missing is a sharp onset in the optical conductivity, as expected for a sharp energy gap. Infrared spectroscopy performed by David Tanner's group on our samples indicates the presence of a transmission peak around 700cm^{-1} , corresponding to $12 k_B T_c$ (Romero *et al.* 1991). This feature is due to a smooth onset of the optical conductivity, and can be well interpreted in terms of a two component model (by assuming a temperature dependent Drude contribution and temperature independent oscillators in the mid-infrared band), or in a single component picture (assuming frequency dependent relaxation rate and effective mass in the normal state and a low frequency depression in σ_1 in the superconducting state). One is tempted to associate this high frequency feature in the optical transmission with the peak in the tunneling density of states at 38meV (Mandrus *et al.* 1993b). However, in the absence of a comprehensive theory, this assignment can be made only tentatively.

Tunneling, in principle, is capable of exploring the anisotropic gap directly. For ideal planar junctions the tunneling probability is a strong function of the incidence angle of the electrons, effectively eliminating non-perpendicular the momentum states (coherent tunneling, (Wolf 1985)). Therefore the "tunneling DOS" is often different from the real DOS. To elucidate the difference between the two quantities, we write the DOS in the form of

$$N(E) = \sum_{\mathbf{k}} A(\mathbf{k}, E) \approx \sum_{\mathbf{k}} \delta(\epsilon_{\mathbf{k}} - E) \quad (5)$$

where \mathbf{k} and $\epsilon_{\mathbf{k}}$ are momentum and the energy of the electrons, and $A(\mathbf{k}, E)$ is the spectral function and the sum runs over all \mathbf{k} values in the Brillouin zone. The tunneling DOS can be well approximated by a similar sum, with the constraint that the allowed \mathbf{k} values are all perpendicular to the junction surface. The distinction between the two quantities is important for planar junctions made on single crystal samples. The real DOS corresponds to an angular average of the tunneling DOS functions.

If we apply these ideas to anisotropic s -wave or to d -wave superconductivity, we find that coherent tunneling should result in fully "gapped" tunneling curves, with a gap value depending on the particular direction of the break. Although we see a major difference between the c -axis and a - b plane tunneling, we do not find significant difference within the a - b plane (the junctions prepared in random directions perpendicular to the CuO layers provide similar tunneling characteristics). The most likely explanation is that the junction surface is rugged or small, and the tunneling momentum spreads over a wide range of angles within the a - b plane. The absence of the Fraunhofer pattern in the magnetic field dependence of the Josephson current points to this explanation. A more exotic possibility is that the lobes of the gap function are not fixed in space and time, providing angular averaging by fluctuations. Finally, it is possible that the superconductivity is truly gapless; the density of states is isotropic and finite, with a value very close to zero at $E=0$ (*i.e.* at the Fermi level).

In summary, the tunneling and optical data do not show evidence for an isotropic gap within the a - b planes of $\text{Bi}_2\text{Sr}_2\text{CaCu}_2\text{O}_8$. In our first reports we stated: "a major result of our investigation is the absence of observable superconducting gap" (Forro *et al.* 1990a) and "the data indicate non-zero DOS at energies different from the Fermi energy" (Mandrus *et al.* 1991a). The results presented here lend further support to those conclusions.

ACKNOWLEDGEMENTS

We are indebted to G.P. Williams, C.J. Hirschmugl and G.L. Carr for valuable assistance in performing and evaluating the infrared measurements, to M. Gurvitch for discussions on the tunneling results and to D.B. Tanner for comments on the optical data. This work was supported by the NSF grant DMR 9016456; the experiments in Brookhaven were supported by the Department of Energy. LF acknowledges support by the FNSRS, grant # 4030-032779.

REFERENCES:

- * Present address: Physics Division, Los Alamos National Laboratory, Los Alamos, NM
- + Permanent address: Institute of Physics of the University, Zagreb, Croatia
- T. Becherer *et al.* Z. Phys. B **86**, 23 (1992)
- W.F. Brinkman, R.C. Dynes and J.M. Rowell, J. Appl. Phys. **41**, 1915 (1970)
- E. Burstein, S. Lundqvist, Tunneling Phenomena in Solids, Plenum, New York, 1969, p. 43.
- D.A. Bonn *et al.* Phys. Rev. Letters, **68**, 2390 (1992)
- L. Forro, G.L. Carr, G.P. Williams, D. Mandrus and L. Mihaly, Phys. Rev. Letters, **65**, 1941 (1990a)
- L. Forro, D. Mandrus, R. Reeder, B. Keszzi and L. Mihaly, J. Appl. Phys., **68**, 4876 (1990b)
- L. Forro, D. Mandrus, C. Kendziora, L. Mihaly and R. Reeder, Phys. Rev. B **42**, 8704 (1990c)
- K. Kamaras, S.L. Herr, C.D. Porter, N. Tache, D.B. Tanner, S. Etemad, T. Vankatesan, E. Chase, A. Inam, X.D. Wu, M.S. Hedge and B. Dutta, Phys. Rev. Letters, **64**, 84 (1990)
- C. Kendziora *et al.* Phys. Rev. B, **45**, 13025 (1992)
- J.R. Kirtley and D.J. Scalapino, Phys. Rev. Letters, **65**, 798, (1990)
- P.B. Littlewood and C.M. Varma, Phys. Rev. B **45**, 12636 (1992)
- D. Mandrus, L. Forro, D. Koller and L. Mihaly, Nature, **351**, 460 (1991a)
- D. Mandrus, L. Forro, C. Kendziora, L. Mihaly, Phys. Rev. B, **44**, 2418 (1991b)
- D. Mandrus, M.C. Martin, C. Kendziora, D. Koller, L. Forro, and L. Mihaly, to be published in Phys. Rev. Letters (1993a)
- D. Mandrus, J. Hartge, C. Kendziora, L. Mihaly and L. Forro, to be published in Europhysics Letters (1993b)
- F. Mezei and A. Zawadowski, Phys. Rev. B, **3**, 3127 (1971)
- J. Moreland and J.W. Ekin, J. Appl. Phys. **58**, 3888 (1985)
- C.J. Muller, J.M. van Ruitenbeek and L.J. de Jongh, Physica C **191**, 485 (1992)
- M.C. Nuss, P.M. Mankiewich, M.L. O'Malley, E.H. Westerwick, P.B. Littlewood, Phys. Rev. Letters, **66**, 3305, (1991)
- D.C. Ralph and R.A. Buhrman, Phys. Rev. Letters, **69**, 2118 (1992)
- D.B. Romero *et al.* Phys. Rev. Letters, **68**, 1590 (1992)
- D.B. Romero, G.L. Carr, D.B. Tanner, L. Forro, D. Mandrus, L. Mihaly, G.P. Williams, Phys. Rev. B **44**, 2818 (1991)
- D.B. Tanner *et al.* in "High Temperature Superconductivity" ed. J. Ashkenazi *et al.* Plenum, New York (1991)
- M. Tinkham, Introduction to superconductivity, McGraw-Hill, New York, 1975
- E.L. Wolf, Principles of Electron Tunneling Spectroscopy, Oxford University Press, New York, 1985;
- Zawadowski (1993) private communication